nature chemistry

ARTICLES

PUBLISHED ONLINE: 4 JULY 2010 | DOI: 10.1038/NCHEM.722

Electrically induced bonding of DNA to gold

Matthias Erdmann[1], Ralf David[2], Ann R. Fornof[1]* and Hermann E. Gaub[1]

The development of single-molecule techniques has afforded many new methods for the observation and assembly of supramolecular structures and biomolecular networks. We previously reported a method, known as the single-molecule cut-and-paste approach, to pick up and deposit individual DNA strands on a surface. This, however, required pre-functionalization of the surface with DNA strands complementary to those that were to be picked up and then deposited. Here we show that single molecules of double-stranded DNA, bound to the tip of an atomic force microscope, can be deposited on a bare gold electrode using an electrical trigger (surface potential cycling). The interactions between the DNA and the electrode were investigated and we found that double-stranded DNA chemisorbs to the gold electrode exclusively at its end through primary amine groups. We corroborated this finding in experiments in which only a single adenosine nucleotide on a polyethylene glycol spacer was 'electrosorbed' to the gold electrode.

The rapid development of novel experimental tools that allow the precise application and measurement of minute forces has opened exciting new possibilities in material and life sciences. Specifically, the swiftly growing family of single-molecule techniques has provided novel routes with which to assemble and probe supramolecular structures and biomolecular networks[1]. A prominent example is the single-molecule cut-and-paste approach[2–4], which combines the precision of atomic force microscopy (AFM) with the selectivity of DNA hybridization to deliver individual molecules to a target zone. In this approach, a DNA strand is picked up from a 'depot' with an AFM tip functionalized with a complementary DNA strand. The cargo DNA can then be transported precisely by the AFM tip to a target zone, where it can be released upon hybridization with a surface-bound DNA strand. Differences in the selected lengths and binding geometries of the DNA oligomers are used to tune the (un)binding forces between the complementary depot/target/cargo strands on hybridizing with oligomers attached to the AFM tip. The binding force between the target DNA and the cargo DNA is larger that the binding force between the functionalized AFM tip and the cargo DNA, which is in turn larger than that between the depot DNA and the cargo DNA. This passive hierarchy of interaction forces between different DNA strands dictates whether or not a molecule is delivered, but it would be highly desirable to be able to covalently attach the cargo molecule directly to the surface using an external parameter such as a voltage pulse, rather than requiring a pre-functionalized surface. The delivery and anchoring of single molecules to a chosen position on the surface could then be controlled electrochemically with a push of a button, rendering conventional surface functionalization protocols unnecessary. Many other applications are conceivable in which such an electrosorption of DNA to gold could be useful, for example in biochip sensors or similar products[5–7]. DNA-templated metal wire formation or the surface attachment of DNA 'origami' structures are other prominent examples in which a triggered chemical attachment of DNA would be of great advantage[8–13].

Results and discussion

Electrosorbing single double-stranded DNA molecules to a gold electrode. A wealth of experimental data are available about DNA in electric fields at surfaces, for example in relation to potentiometric and amperometric sensors, nanodevices and other technological applications[14–20]. AFM-based single-molecule force spectroscopy seems a natural choice to investigate the interaction of DNA with surfaces, and cyclic voltammetry is the established technique for analysing and controlling the electrochemistry of gold as a function of its potential[21–24]. We used a combination of both of these techniques in this study (see Fig. 1). We covalently attached one strand of double-stranded DNA (dsDNA) to the tip of the AFM cantilever by thiol/peptide chemistry (see Supplementary Information). We then adjusted the surface potential of a 100-μm gold microelectrode using potentiostatic control with respect to a Ag/AgCl reference electrode. At 0 V the tip was moved to the surface. No measurable interaction was recorded on approach or on retraction. The tip was then kept 200 nm above the surface while the potential was ramped to −1 V and back to 0 V. Upon retracting the tip, a force–extension trace with all of the typical features of a single molecule of dsDNA was recorded: entropic elasticity followed by a plateau at 65 pN (refs 25–27). This feature, known as the B–S plateau, distinguishes the B to S transition, whereby the dsDNA is stretched at constant force from its natural B-state to the overstretched S-state, with the dsDNA lengthened by a factor of 1.7. Further stretching leads to higher forces and an unbinding of the overstretched strand. At the end of this unbinding transition, at ~180 pN, the two strands separate. The measured force increase of up to 270 pN is therefore a strong indication that the strand that was covalently attached to the tip has established a stable interaction with the gold surface during the potential sweep. It is the terminal segment of the dsDNA that interacts with the gold surface, rather than the entire backbone adhering to the surface, as indicated by the pronounced B–S plateau, which is observed to have the standard force of 65 pN, and by the fact that no additional interaction between the dsDNA backbone and the gold surface was measured.

Force–extension curves with stepwise potential change. To investigate the potential at which this electrically induced attachment occurred, we performed single-molecule force spectroscopy scans with a speed of 1.5 μm s^{-1} while ramping the surface potential in steps of 9 mV (see Fig. 2)[28] after each force–extension curve. For these prolonged scans we had to increase the functionalization density of the tip at the cost of multiple DNA

[1]Center for NanoScience, Ludwigs-Maximilians-Universität Munich, Amalienstrasse 54, 80799 Munich, [2]Center for Integrated Protein Science Munich, Department of Chemistry and Biochemistry, Butenandtstrasse 5-13, 81377 Munich, Germany. *e-mail: ann.fornof@physik.uni-muenchen.de

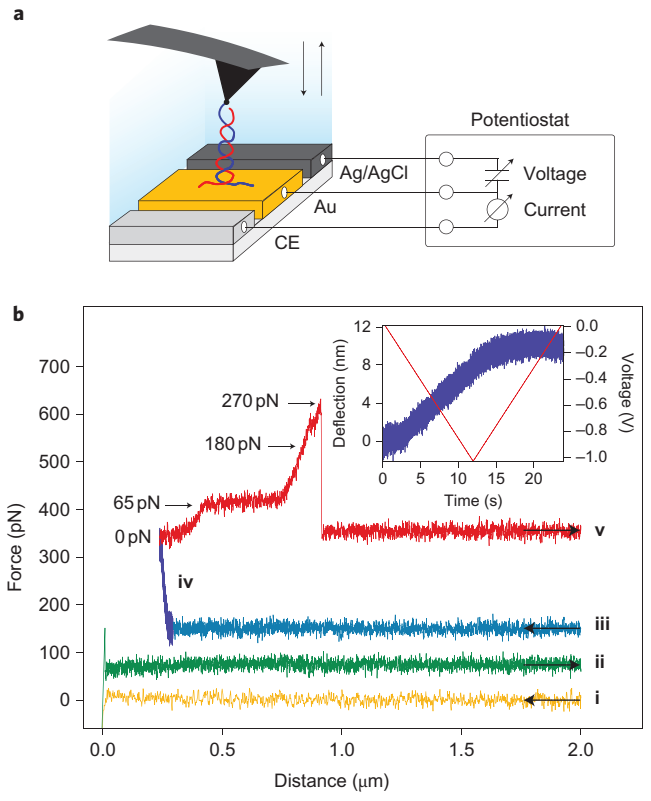

Figure 1 | Electrically induced chemical bonding of a dsDNA strand to gold through its terminal end. a, Schematic representation of the AFM experiments on a polarized gold electrode. dsDNA was covalently bound to an AFM tip and brought into contact with a bare gold microelectrode. The surface potential of the gold electrode versus a Ag/AgCl reference electrode was controlled by a potentiostat through a platinum counter electrode (CE). **b**, Force–extension curves show the electrosorption of a dsDNA molecule to the surface. At zero potential, the AFM tip was brought into contact with the surface and was retracted (**i**, **ii**). The tip was then kept 200 nm above the surface (**iii**) while the potential was changed from 0 V to −1 V and back to 0 V with a sweep rate of 85 mV s^{-1} (**iv**). Finally, the behaviour of the dsDNA was monitored as the tip was retracted completely: stretching of the dsDNA molecule, followed by the B-S transition, the melting of the DNA and finally the complete detachment of the DNA (**v**). Inset: drift and crosstalk of the potential sweep (red curve) into the deflection signal (blue curve) caused by the polarization currents, demonstrating that the tip and gold surface were not in contact while the DNA was 'electrosorbed' to the surface.

interactions during contact. However, with a higher tip functionalization density we increased the storage capacity of the tip and were able to complete several voltammetric cycles with the same tip. Nevertheless, we were able to resolve the rupture force of individual DNA molecules by analysing only the last step in the force curves. In addition, we were able to quantify the loss of functionalized dsDNA molecules from the AFM tip to the surface (we call this the 'wear-out' of the tip) by analysing the number of molecules interacting with the surface with time.

The most remarkable, and at first counterintuitive, feature is the asymmetric distribution in the measured values of rupture force at negative potentials (Fig. 2b). Both the distribution and magnitude of the rupture force values were persistent over several cycles, but this was not the case for the number of interacting molecules, which decreased constantly from cycle to cycle (Fig. 2c). To gain further insight into the electrochemistry of this process we plotted the rupture forces against potential in the same format used in cyclic voltammetry and named these plots roburograms (*robur* means force in Latin) (Fig. 2d). The well-known oxidation and reduction peaks of the gold electrode are pronounced in the cyclic voltammogram and mark the borders of the window in which measurable values of rupture force were found[22,29]. This gives the first clear hint that only a reduced gold surface binds DNA. But why is the negatively charged DNA not repelled by the negatively polarized gold electrode? The strong hysteresis of the roburogram indicates that the interaction of the DNA with the gold surface has a pronounced memory. The explanation is summarized in Fig. 2e: at positive potentials the gold surface is oxidized and not reactive. At negative potentials Mg^{2+} ions migrate to the gold electrode and increasingly cover the gold surface. When the gold-coated tip touches the gold surface, the electrical contact (contact resistance of 40 Ω) short-circuits the electric field in the contact zone, and the positive charge of the Mg^{2+} ions attracts the DNA to the gold electrode. Even when the scan direction is reversed, the potential is still negative and an increasing number of Mg^{2+} ions are accumulated on the electrode, thereby increasing the attraction and increasing the likelihood for multiple bonds to form[30]. As a consequence, the rupture force increases until oxidation sets in, rendering the electrode non-reactive again.

Nucleotide-specific DNA–gold-surface interactions through coordinate N–Au bonding. As yet, we have not discussed the reactive species on the DNA. It is well known that the ends of dsDNA are not static but tend to open up along several base pairs in a highly dynamic manner[31,32]. It is thus likely that the bases at the end come into contact with the gold surface. These bases have primary amine groups with the exception of thymine. In previous experiments we learned that a slightly basic pH, which is created through hydrolysis at negative potentials[33], is required for bonding. It is thus conceivable that the amines interact with under-coordinated, reduced gold atoms and form a coordination bond[34–37]. To test this hypothesis we performed the same experiment as before, but now with a set of constructs that had systematically altered base-pair sequences at the end, which were then exposed to the gold surface.

As outlined in Fig. 3, we expect that if the strand that is covalently attached to the tip chemisorbs to the gold surface at the other end, this coordinate bond will rupture at elevated forces. The dsDNA may be stretched through the B–S transition, but the counterstrand will remain at least loosely attached to the strand under tension so that, in repeated experiments, the coordinate bond may be formed again. We were able to promote this geometry by adding a fivefold adenosine sequence to a heterogeneous dsDNA (TA-dsDNA).

In the case where the counterstrand chemisorbs to the surface, however, both strands are split apart upon retraction[38–40]. One single-stranded DNA (ssDNA) stays at the tip, the other on the gold surface. ssDNA is known to strongly interact with both the tip and the gold surface, so re-annealing of the DNA is very unlikely[41,42]. This would result in an increasing deposition of ssDNA on the surface and, therefore, a rapidly decreasing number of observed bond formations between the amine functionality of the dsDNA on the tip and the gold atoms at the electrode surface. To promote this shear geometry, the fivefold adenosine sequence was also added to the counterstrand. For a direct comparison between these two constructs (and several others described in the Supplementary Information), the number of rupture events was recorded during a full cycle, in close analogy to the protocol in Fig. 2. The wear-out of the tip was found to be extremely high in the case of AT-dsDNA, whereas the TA-dsDNA revealed ten times higher stability than the AT-dsDNA over the five subsequent potential cycles. The non-sequence-specific component of AFM tip wear-out (during more than 2,500 force–distance cycles) may be due to mechanical damage to any part of the construct attaching the DNA

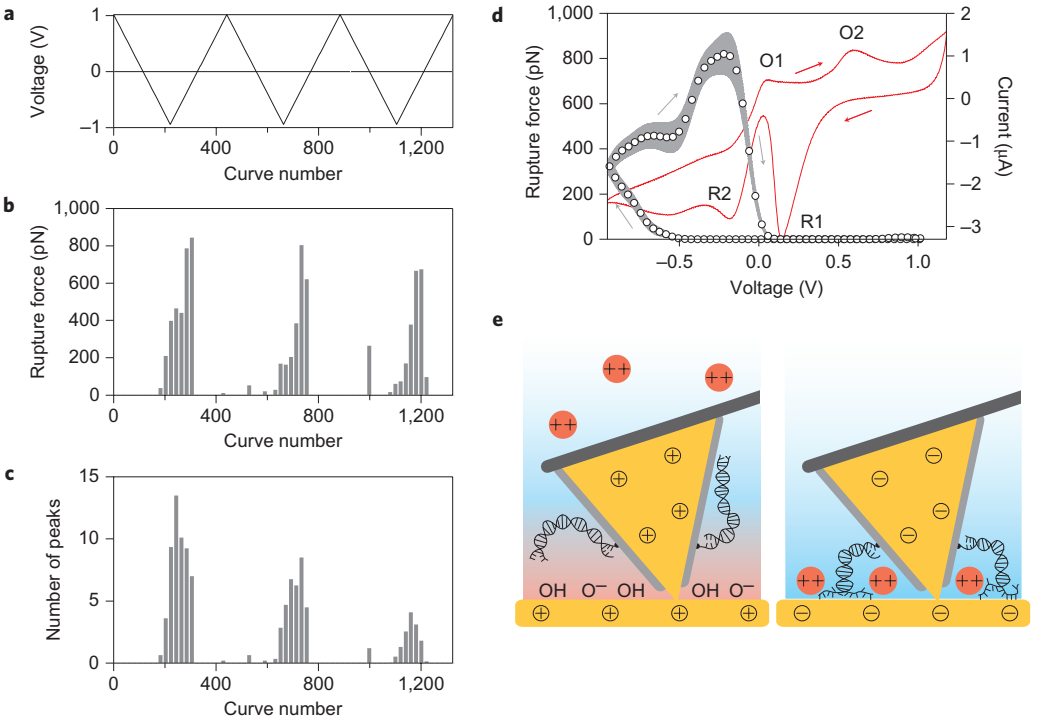

Figure 2 | Electrochemistry of DNA-gold bonding. a, The potential of the gold electrode was ramped between −1.0 and 1.0 V in 9 mV steps while recording a force–extension curve with a speed of 1.5 μm s^{-1}. **b**,**c**, Plots showing the magnitude of the last step in the force curve, which results from a single molecule detachment (**b**) and the overall number of rupture peaks throughout the force curve, reflecting the number of bound molecules (**c**). Molecules of dsDNA were bound to the gold electrode at potential values around −1 V, resulting in rupture forces up to 800 pN. Although the asymmetric rupture force distribution was constant over several cycles, the number of bound molecules decreased, indicating a loss of functionalized dsDNA molecules from the AFM tip to the surface. **d**, Rupture force values plotted against potential in the same format as in cyclic voltammetry ('roburograms'). The binned and smoothed rupture forces values (circles; grey error region indicates the interpolated standard error of the mean) were evaluated with the polarization current (red) and plotted in a cyclic voltammogram (recorded at 100 mV s^{-1}). Indicated are the well-known oxidation and reduction peaks of the gold surface (O1, O2, R1 and R2). **e**, Left: positive potentials prevent DNA electrosorption due to an oxidized gold surface and an acidic microenvironment (red). Right: negative potentials induce DNA electrosorption due to a reduced gold surface, adsorbed Mg^{2+} ions (red circles) and a basic microenvironment (blue).

to the tip, but may also reflect the possibility that bases beyond the terminal pentamer occasionally interact with the gold surface. For a detailed discussion and additional data on the chemisorption of various DNA constructs, see Supplementary Information. Because thymidine is the only nucleotide without a primary amine, these results clearly show that the primary amines on the bases at the end of the DNA bind to the gold surface.

Measurement of an electrically induced single N–Au bond. We speculated in the beginning that multiple bonds may be the cause of the wide distribution of the measured rupture forces. To test this assumption we attached different single nucleotides to the tip with PEG spacers and measured the rupture forces for several potentials (Fig. 4). We found no measurable interaction for thymidine, regardless of the potential. For adenosine we found clear single-molecule stretching signatures in the force scans and rupture forces, which were virtually indistinguishable for the different potentials. The mean force values of 170 pN varied by less than 15 pN, whereas the half-width of the histograms was more than 50 pN. Those histograms (depicted in Fig. 4c) show a rather broad distribution with an asymmetric shape. The broad distribution is not surprising if one takes into account that the gold surface is rough and heterogeneous at the atomic level and that different adsorption geometries involving different atoms from the DNA base are possible. The mean value can be rationalized by a simple estimate; with typical energies reported for the Au–N bond of 32–42 kJ mol^{-1} and estimated bond lengths of 0.3 nm one would expect a barrier force of 185 pN to be a realistic estimate[43,44]. The literature values for adhesion enthalpies for DNA bases on different gold surfaces and different solvents range from 32 to 140 kJ mol^{-1} (refs 45–47, using different methods). It is important to note, however, that the adhesion enthalpies result from a superposition of different kinds of interactions, in our case mainly short-range chemical interactions and long-range van der Waals interactions. The chemical interactions decay exponentially over a few Angstroms, whereas the van der Waals interactions decay with a (d^{-3}) law over several nanometres[48]. As a result, the adhesion forces, which follow the potential gradient, are dominated by the short-range interactions. We therefore made our estimate based on the enthalpy values derived from density functional theory (DFT) calculations, because those come closest to the interactions probed by force[43]. It is interesting to note that several studies report a lower adhesion enthalpy for thymine than for the other bases[45,49]. If one takes into account that the van der Waals contribution of the four bases is expected to be comparable, this finding supports our result, that thymine is lacking the contribution of the coordination bond. This in turn points towards the main strength of single-molecule force spectroscopy: to discriminate between the different contributions of an interaction. Furthermore, our results indicate that the rupture force of the coordinate bond is largely independent of potential (Fig. 4b) and that the higher rupture forces found in the DNA experiments stem from multiple bases electrosorbed to the gold surface, modulated also by the different surface geometries of the bonds. The formation of such a bond, however, was found to be sensitively dependent on the electrochemistry at the surface.

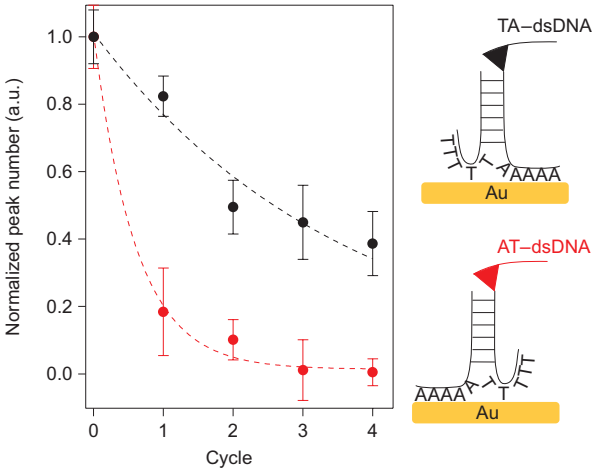

Figure 3 | Nucleotide specificity of DNA–gold electrosorption. dsDNA was covalently attached to the tip by only one strand, which bears at the other end either five adenosines (A) or 5 thymidines (T) and the experiment summarized in Fig. 2 was repeated. Note that A has a primary amine but T does not. The number of rupture peaks was then summed throughout a complete cycle, normalized, and plotted versus the cycle number—error bars indicate the normalized standard error of the mean of integrated peak distributions per cycle. Both curves show a wear-out of the functionalization but reveal a drastic increase of wear-out by roughly an order of magnitude for the AT-dsDNA. Because the covalent bonds of the attachment chemistry and the DNA backbone are stronger than the coordinate bond, the latter will rupture with higher probability and repetitive electrosorption is possible (black trace). In contrast, if the counterstrand is chemisorbed, the two strands will split apart upon pulling. ssDNA is known to strongly interact with the tip surface, so the likelihood of re-hybridization is strongly reduced, and the number of reactive molecules decays rapidly (red trace). These results, together with all of the controls (see Supplementary Information), strongly indicate that the primary amine of the bases forms a coordinate bond with the gold surface during electrosorption.

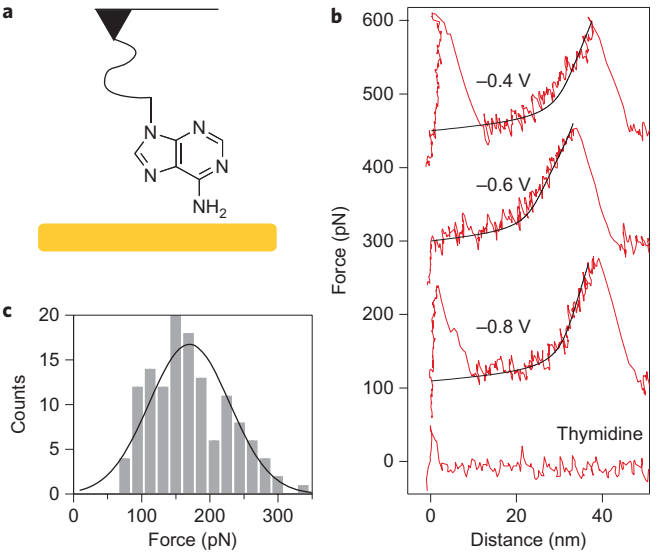

Figure 4 | Coordination bond rupture of individual nucleotides. a, Single nucleotides were attached to the AFM tip through 10 kDa PEG spacer molecules **b**, Typical examples of force–extension curves, with adenosine (upper three traces) and thymidine (lower trace) were recorded at constant potentials ranging from −0.4 to −1 V. No measurable interaction could be observed for thymidine, but for adenosine, the stretching of the PEG spacer (two-state freely-jointed-chain (FJC) fit, black curve) and the rupture of the N–Au bond at about 180 pN could be repeatedly observed. No marked difference was found between the three different potentials. **c**, Corresponding histogram of 135 force–extension curves, showing an average rupture force of 170±50 pN.

Conclusions

Control of the parameters described above thus enables us to electrochemically bond individual DNA strands to gold surfaces by attachment at their ends. Single-molecule contacts can be guided to chosen positions and stably attached by an electrical trigger, much like bonding a wire to a contact. With the enormous range of applications for DNA both as a key biomolecule and, increasingly, as a programmable nanoscale building block, this option of electrically inducing the chemisorption of individual DNA strands and defining their positions on a surface using the precision of AFM will find an abundance of novel applications.

Material and Methods

AFM. We used a commercial instrument (Molecular Force Probe 3D, Asylum Research) and silicon nitride cantilevers (Veeco). The spring constants of each cantilever were individually calibrated by thermal calibration. Moreover, a PEEK-cantilever holder from Asylum Research was used to avoid the requirement for additional metal parts in the solution.

Samples. dsDNA fragments of 4.9 kbp (~100 ng μl^{-1} concentration) were obtained by polymerase chain reaction (PCR) with Fusion polymerase (Finnzymes) using a pet28a-vector (Novagen, Merck Biosciences) as a template, 5′-amino-modified forward primer, and a corresponding reverse primer from IBA. The dsDNA was purified with the Qiagen PCR Purification Kit. Agarose gel electrophoresis was used to confirm the homogeneity of the DNA length.

For the TA-, AT-, GC- and CG-dsDNA the corresponding reverse primers were elongated at the 5′-end by an additional five homogeneous bases A, T, C or G. The overhangs were filled by the polymerase with complementary bases during amplification. To generate a five A or T single-strand overhang a hexaethylene glycol spacer was inserted between the reverse primer and the A or T overhang to avoid filling with complementary bases.

Experiments were performed in 50 μM $MgCl_2$ and chromatography water (LiChrosolv, Merck) containing traces of NaOH or HCl to ensure pH values of 5.5, 8.5 or 10. All chemicals were purchased from Sigma Aldrich and used as received if not otherwise identified.

Tip functionalization. The covalent attachment of dsDNA to the AFM tip was accomplished through the reaction between an activated carboxylic acid on the tip and a primary amine from the primer on the dsDNA. To accomplish this binding chemistry, the cantilevers were coated with a 30 Å chrome/nickel (80:20) layer followed by a 300 Å layer of gold by thermal evaporation. These cantilevers were then etched for 2 min in a solution containing H_2O (Milli-Q water), NH_3 (37%) and H_2O_2 (30%) at a ratio of 10:1:1 and then rinsed with ethanol (puriss.). Afterwards, the cantilevers were immediately incubated in a solution of 16-mercaptohexadecanoic acid (0.5 mM), 11-mercaptoundecanol (0.5 mM) and *tris*(2-carboxyethyl)phosphine-hydrochloride (TCEP, 0.05 mM) in ethanol (puriss.) for at least 12 h. For experiments with a dilute dsDNA functionalization (Fig. 1), the concentration of 16-mercaptohexadecanoic acid was 0.05 mM. For dsDNA functionalization, the cantilevers were first rinsed in chromatography water (LiChrosolv, Merck). The carboxylic acid groups of the SAM were then reacted with the amino end groups of the dsDNA in a solution of 10 μl DNA and 20 μl chromatography water containing 1-ethyl-3-(3-dimethylaminopropyl) carbodiimide (EDC) for 30 min. EDC (15 mg) was dissolved in 300 μl chromatography water for the latter stock solution. The large excess of EDC enabled carboxy-amino coupling in the polar solution; the use of chromatography water ensured constant coupling conditions at pH 7. After functionalization, the cantilevers were rinsed thoroughly in the $MgCl_2$ solution and then immediately used in the experiments. Depending on the 16-mercaptohexadecanoic acid concentration, approximately 10–30 dsDNA molecules (0.5 mM) or 1–3 dsDNA molecules (0.05 mM) could be determined in the corresponding force–extension curve.

The functionalization of 10 kDa PEG and single nucleotides to the AFM tip was accomplished with two different protocols, one already published[2] and the other a new protocol. The effective weight of the commercial 10 kDa PEG spacer was measured by mass spectrometry, which gave a value of 8.2 kDa or a contour length of 54 to 60 nm. As it is likely that the molecule is not attached directly at the apex of the AFM tip, the effective length of the PEG may be shorter than expected from matrix assisted laser desorption/ionization time of flight (MALDI-TOF) results.

Electrodes. The gold electrodes were directly evaporated on a clean polycarbonate slide and had an area of 0.1 mm × 20 mm plus an area of 1 cm^2 for electrical

contacting. The thickness of the electrode was 200 nm. A mask of stainless steel (Ätztechnik Herz) was used during thermal evaporation. Before use in the experiment, the electrodes were first rinsed with ethanol (puriss.), Milli-Q water and the $MgCl_2$ solution. The electrodes were then dried with nitrogen to ensure a dry contacting area for BNC (Bayonet Neill-Concelman) cables. For a three-electrode set-up, a commercial Ag/AgCl microelectrode (Microelectrodes) was used as the reference electrode and a platinum wire as the counter electrode. All potentials applied to the gold electrodes are given versus the Ag/AgCl electrode. The counter and reference electrodes were inserted into a bare cavity, which was milled into the polycarbonate slide before functionalization. The $MgCl_2$ solution was then added to determine an effective electrode area of 0.1 mm × 5 mm covered by the solution. Before the AFM experiment, 20 cleaning voltammograms in the range of $\pm$1.2 V were recorded with a sweep rate of 0.1 V s^{-1}.

Received 2 December 2009; accepted 17 May 2010; published online 4 July 2010

References

1. Duwez, A. S. *et al.* Mechanochemistry: targeted delivery of single molecules. *Nature Nanotech.* **1,** 122–125 (2006).
2. Kufer, S. K., Puchner, E. M., Gumpp, H., Liedl, T. & Gaub, H. E. Single-molecule cut-and-paste surface assembly. *Science* **319,** 594–596 (2008).
3. Puchner, E. M., Kufer, S. K., Strackharn, M., Stahl, S. W. & Gaub, H. E. Nanoparticle self-assembly on a DNA-scaffold written by single-molecule cut-and-paste. *Nano Lett.* **8,** 3692–3695 (2008).
4. Kufer, S. K. *et al.* Optically monitoring the mechanical assembly of single molecules. *Nature Nanotech.* **4,** 45–49 (2009).
5. Boon, E. M., Ceres, D. M., Drummond, T. G., Hill, M. G. & Barton, J. K. Mutation detection by electrocatalysis at DNA-modified electrodes. *Nature Biotechnol.* **18,** 1096–1100 (2000).
6. Wang, J. From DNA biosensors to gene chips. *Nucleic Acids Res.* **28,** 3011–3016 (2000).
7. McKendry, R. *et al.* Multiple label-free biodetection and quantitative DNA-binding assays on a nanomechanical cantilever array. *Proc. Natl Acad. Sci. USA* **99,** 9783–9788 (2002).
8. Kershner, R. J. *et al.* Placement and orientation of individual DNA shapes on lithographically patterned surfaces. *Nature Nanotech.* **4,** 557–561 (2009).
9. Braun, E., Eichen, Y., Sivan, U. & Ben-Yoseph, G. DNA-templated assembly and electrode attachment of a conducting silver wire. *Nature* **391,** 775–778 (1998).
10. Winfree, E., Liu, F. R., Wenzler, L. A. & Seeman, N. C. Design and self-assembly of two-dimensional DNA crystals. *Nature* **394,** 539–544 (1998).
11. Rothemund, P. W. K. Folding DNA to create nanoscale shapes and patterns. *Nature* **440,** 297–302 (2006).
12. Marszalek, P. E., Greenleaf, W. J., Li, H. B., Oberhauser, A. F. & Fernandez, J. M. Atomic force microscopy captures quantized plastic deformation in gold nanowires. *Proc. Natl Acad. Sci. USA* **97,** 6282–6286 (2000).
13. Yurke, B., Turberfield, A. J., Mills, A. P., Simmel, F. C. & Neumann, J. L. A DNA-fuelled molecular machine made of DNA. *Nature* **406,** 605–608 (2000).
14. Tao, N. J., Derose, J. A. & Lindsay, S. M. Self-assembly of molecular superstructures studied by in situ scanning tunneling microscopy—DNA bases on Au(111). *J. Phys. Chem.* **97,** 910–919 (1993).
15. Wang, J. *et al.* Sequence-specific electrochemical biosensing of M-tuberculosis DNA. *Anal. Chim. Acta* **337,** 41–48 (1997).
16. Daniel, M. C. & Astruc, D. Gold nanoparticles: assembly, supramolecular chemistry, quantum-size-related properties, and applications toward biology, catalysis, and nanotechnology. *Chem. Rev.* **104,** 293–346 (2004).
17. Fan, F. R. F. & Bard, A. J. STM on wet insulators—electrochemistry or tunneling. *Science* **270,** 1849–1851 (1995).
18. Drummond, T. G., Hill, M. G. & Barton, J. K. Electrochemical DNA sensors. *Nature Biotechnol.* **21,** 1192–1199 (2003).
19. Murphy, L. Biosensors and bioelectrochemistry. *Curr. Opin. Chem. Biol.* **10,** 177–184 (2006).
20. Frederix, P. *et al.* Atomic force bio-analytics. *Curr. Opin. Chem. Biol.* **7,** 641–647 (2003).
21. Rief, M., Clausen-Schaumann, H. & Gaub, H. E. Sequence-dependent mechanics of single DNA molecules. *Nature Struct. Biol.* **6,** 346–349 (1999).
22. Angersteinkozlowska, H., Conway, B. E., Hamelin, A. & Stoicoviciu, L. Elementary steps of electrochemical oxidation of single-crystal planes of Au .1. chemical basis of processes involving geometry of anions and the electrode surfaces. *Electrochim. Acta* **31,** 1051–1061 (1986).
23. Hansma, H. G., Laney, D. E., Bezanilla, M., Sinsheimer, R. L. & Hansma, P. K. Applications for atomic-force microscopy of DNA. *Biophys. J.* **68,** 1672–1677 (1995).
24. Anselmetti, D. *et al.* Biological-materials studied with dynamic force microscopy. *J. Vac. Sci. Technol. B* **12,** 1500–1503 (1994).
25. Bustamante, C., Marko, J. F., Siggia, E. D. & Smith, S. Entropic elasticity of lambda-phage DNA. *Science* **265,** 1599–1600 (1994).
26. Marko, J. F. & Siggia, E. D. Stretching DNA. *Macromolecules* **28,** 8759–8770 (1995).
27. Smith, S. B., Cui, Y. J. & Bustamante, C. Overstretching B-DNA: the elastic response of individual double-stranded and single-stranded DNA molecules. *Science* **271,** 795–799 (1996).
28. Christie, J. H. & Lingane, P. J. Theory of staircase voltammetry. *J. Electroanal. Chem.* **10,** 176–182 (1965).
29. Hamelin, A., Sottomayor, M. J., Silva, F., Chang, S. C. & Weaver, M. J. Cyclic voltammetric characterization of oriented monocrystalline gold surfaces in aqueous alkaline-solution. *J. Electroanal. Chem.* **295,** 291–300 (1990).
30. Pastre, D. *et al.* Adsorption of DNA to mica mediated by divalent counterions: a theoretical and experimental study. *Biophys. J.* **85,** 2507–2518 (2003).
31. Andreatta, D. *et al.* Ultrafast dynamics in DNA: 'fraying' at the end of the helix. *J. Am. Chem. Soc.* **128,** 6885–6892 (2006).
32. Every, A. E. & Russu, I. M. Influence of magnesium ions on spontaneous opening of DNA base pairs. *J. Phys. Chem. B* **112,** 15261–15261 (2008).
33. Shirahata, S. *et al.* Electrolyzed-reduced water scavenges active oxygen species and protects DNA from oxidative damage. *Biochem. Biophys. Res. Commun.* **234,** 269–274 (1997).
34. Xu, B. Q. & Tao, N. J. J. Measurement of single-molecule resistance by repeated formation of molecular junctions. *Science* **301,** 1221–1223 (2003).
35. Chen, F., Li, X. L., Hihath, J., Huang, Z. F. & Tao, N. J. Effect of anchoring groups on single-molecule conductance: comparative study of thiol-, amine-, and carboxylic-acid-terminated molecules. *J. Am. Chem. Soc.* **128,** 15874–15881 (2006).
36. Venkataraman, L., Klare, J. E., Nuckolls, C., Hybertsen, M. S. & Steigerwald, M. L. Dependence of single-molecule junction conductance on molecular conformation. *Nature* **442,** 904–907 (2006).
37. Grunder, S. *et al.* New cruciform structures: toward coordination induced single molecule switches. *J. Org. Chem.* **72,** 8337–8344 (2007).
38. Strunz, T., Oroszlan, K., Schafer, R. & Guntherodt, H. J. Dynamic force spectroscopy of single DNA molecules. *Proc. Natl Acad. Sci. USA* **96,** 11277–11282 (1999).
39. Morfill, J. *et al.* B–S transition in short oligonucleotides. *Biophys. J.* **93,** 2400–2409 (2007).
40. Ho, D. *et al.* Force-driven separation of short double stranded DNA. *Biophys. J.* **97,** 3158–3167 (2009).
41. Herne, T. M. & Tarlov, M. J. Characterization of DNA probes immobilized on gold surfaces. *J. Am. Chem. Soc.* **119,** 8916–8920 (1997).
42. Storhofff, J. J., Elghanian, R., Mirkin, C. A. & Letsinger, R. L. Sequence-dependent stability of DNA-modified gold nanoparticles. *Langmuir* **18,** 6666–6670 (2002).
43. Bilic, A., Reimers, J. R., Hush, N. S. & Hafner, J. Adsorption of ammonia on the gold(111) surface. *J. Chem. Phys.* **116,** 8981–8987 (2002).
44. Lambropoulos, N. A., Reimers, J. R. & Hush, N. S. Binding to gold(0): Accurate computational methods with application to $AuNH_3$. *J. Chem. Phys.* **116,** 10277–10286 (2002).
45. Demers, L. M. *et al.* Thermal desorption behavior and binding properties of DNA bases and nucleosides on gold. *J. Am. Chem. Soc.* **124,** 11248–11249 (2002).
46. Rapino, S. & Zerbetto, F. Modeling the stability and the motion of DNA nucleobases on the gold surface. *Langmuir* **21,** 2512–2518 (2005).
47. Manohar, S. *et al.* Peeling single-stranded DNA from graphite surface to determine oligonucleotide binding energy by force spectroscopy. *Nano Lett.* **8,** 4365–4372 (2008).
48. Israelachvili, J. *van der Waals Forces between Surfaces* 2nd edn, II (Academic, 2003).
49. Ostblom, M., Liedberg, B., Demers, L. M. & Mirkin, C. A. On the structure and desorption dynamics of DNA bases adsorbed on gold: a temperature-programmed study. *J. Phys. Chem. B* **109,** 15150–15160 (2005).

Acknowledgements

The authors thank K. Gottschalk, D. Ho, W. Schuhmann and U. Sivan for helpful discussions. This work was supported by the German Science Foundation (SFB 486) and the Nanosystems Initiative Munich (NIM). A.F. thanks the Alexander von Humboldt Foundation for generous support.

Author contributions

M.E., A.F. and H.E.G. conceived and designed the experiments and co-wrote the paper. M.E. performed the experiments and analysed the data. R.D. contributed the dsDNA and provided the tip and electrode functionalization. All authors discussed the results and commented on the manuscript.

Additional information

The authors declare no competing financial interests. Supplementary information accompanies this paper at www.nature.com/naturechemistry. Reprints and permission information is available online at http://npg.nature.com/reprintsandpermissions/. Correspondence and requests for materials should be addressed to A.R.F.